

# Automated eddy detection in the Brazil Current near the Abrolhos Bank (17-21°S)

Gabriel Aarão Gonçalves <sup>1</sup>  
Leonardo Carvalho de Jesus<sup>1</sup>  
Julio Tomas Aquije Chacaltana <sup>1</sup>

<sup>1</sup> Federal University of Espírito Santo, Brazil  
Technological Centre  
Department of Environmental Engineering

June 27, 2018



# Table of contents

- 1 Introduction
- 2 Objective
- 3 Data
- 4 Methodology
  - Eddy detection method
  - Validation of the eddy detection method for the region of study
  - Eddy boundaries, radius and eddy tracking
- 5 Results and discussion
  - Validation of the automated eddy method
  - Eddy detection
  - Eddy radius
  - Eddy shapes
  - Eddy tracking
- 6 Conclusion



# Introduction

- The Brazil Current (BC) is a western boundary current and it has origin in the South Equatorial Current (SEC) bifurcation, which is part of the South Atlantic subtropical gyre (Peterson and Stramma, 1991).

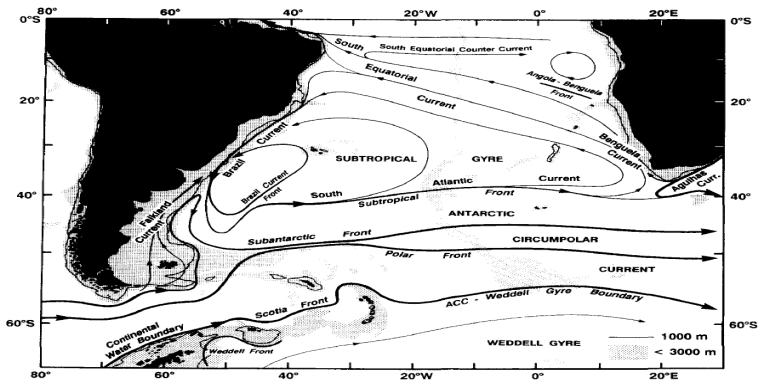


Figure 1: Schematic representation of the large scale circulation in the South Atlantic Ocean. Source: Peterson and Stramma (1991)

# Introduction

- The (BC) in the ocean is characterized by a predominant pattern of meanders and eddies:
  - Cabo Frio region (Signorini, 1978; de Miranda and Castro, 1979);
  - Cape São Tomé (Garfield, 1990; Da Silveira et al., 2008);
  - Vitória (Schmid et al., 1995),
  - Abrolhos, Royal Charlotte and Ilhéus eddies (SOUTELINO, 2008)
- Important role in the transport of momentum and heat, as well in the occurrence of upwelling events (McWilliams, 2008).

# Introduction

- The application of an automated eddy detection method can be useful, especially for the study of eddies from a large dataset.
- Automated eddy detection can be divided in three different categories:

## Categories of automated eddy detection

1. Based on physical parameters;
2. Based on the geometry of the flow;
3. Hybrid: association of both categories (physical and geometric)

- In principle, the **geometric category** is better than the **physical criteria**, because they are based on the properties of a whole region, such as streamlines [Sadarjoen \(1999\)](#) and the physical criteria usually detect eddies that do not correspond to true eddies ([Sadarjoen, 1999](#); [Chaigneau et al., 2008](#)) .
- **Hybrid category**: The work of ([Chaigneau et al., 2008](#)) used a geometric technique for the delimitation of eddy boundary and a physical criteria for the eddy detection.

# Objective

- Apply a geometric eddy detection method for evaluate the eddy characteristics near the Abrolhos Bank.

# Data

- Reanalysis dataset of the consortium HYCOM (*HYbrid Coordinate Ocean Model*) during 2010.

**Table 1:** Specifications of the HYCOM dataset

<b>Data</b>	<b>Specifications</b>
Spatial resolution	1/12.5°
Time intervals	1 day
Latitude	(13-21°S) <sup>1</sup> and (17-21°S) <sup>2</sup>
Longitude	(35-41°W)
Variables	Zonal and meridional component of velocity

<sup>1</sup> Coordinates used for validation of the eddy detection method;

<sup>2</sup> Coordinates of the region of study.



# Region of study

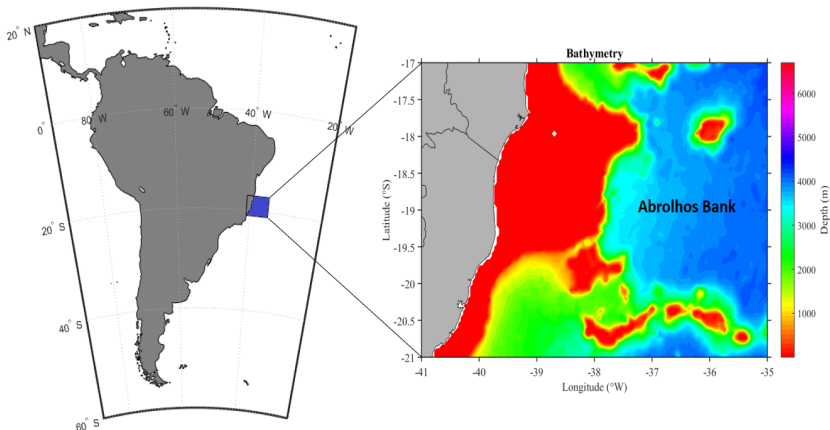


Figure 2: (Left): region of study (blue). (Right): bathymetry of the region of study, indicating the Abrolhos Bank



# Eddy detection method

- Automated eddy detection developed by (Nencioli et al., 2010)
- Eddy centers are determined when 4 constraints are satisfied (Figure 3):
  1. Along an east–west section,  $v$  has to reverse in sign across the eddy center and its magnitude has to increase away from it;
  2. The same for  $u$  in north–south section;
  3. Velocity magnitude has a local minimum at the eddy center;
  4. The directions of the velocity vectors have to change with a constant sense of rotation and the directions of two neighboring velocity vectors have to lay within the same or two adjacent quadrants;
- The constraints depend on two parameters ( $a$  and  $b$ ), that give flexibility to the algorithm:
  - In our study:  $a = 3$  and  $b = 2$

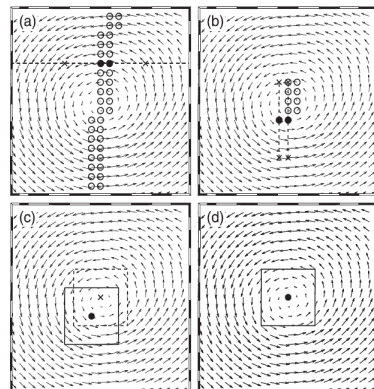


Figure 3: (a) First, (b) second, (c) third, and (d) fourth constraint. Source: Nencioli et al. (2010)

# Validation of the automated eddy method

- Efficiency was validated by two parameters [Chaigneau et al. \(2008\)](#):

$$\text{SDR} = \frac{N_c}{N_e} \quad (1)$$

$$\text{EDR} = \frac{N_{om}}{N_e} \quad (2)$$

- $N_c$ : common eddies identified by both the authors and the automated method;
  - $N_e$ : total number of eddies identified by the authors;
  - $N_{om}$ : eddies identified only by the method.
- 10 days of the dataset were aleatory selected, as well different depths were choosed (between 0 and 400 m).

## Description of the eddy boundaries, radius and tracking

- **Eddy boundary:** defined as the outermost closed streamline around the eddy center, different from the definition of [Nencioli et al. \(2010\)](#). The definition used in our work was also used by [Xia and Shen \(2015\)](#).
  - In cases eddies centers have no closed contours of streamfunction, the eddy shape is assumed to be circular with radius  $a - 1$  grid points (16.5 km) in our data.
- **Eddy radius:** computed as the mean distance between the center of the eddy and all the points defining the contourline adopted as eddy limit.
- **Eddy tracking:** determined comparing the centers at successive time steps, starting from the first day, using a searching area with radius of 25 km.
  - The number of eddy centers found is the eddy lifetime (days).

# Validation of the automated eddy detection for the region of study

Table 2: Validation of the automated eddy detection for the region of study

Day	88344	90912	93336	96504	97704	100272	102360	106632	107016	107304	Total
Depth (m)	400	0	0	50	20	150	200	0	0	0	-
$N_e$	11	7	6	9	8	9	10	4	5	3	72
$N_c$	9	7	6	9	7	9	10	3	5	2	67
$N_{om}$	0	0	0	0	0	0	0	0	0	1	1
Missing eddies	2	0	0	0	1	0	0	1	0	1	5
SDR (%)	81.82	100	100	100	87.50	100	100	75	100	66.67	91.10
EDR (%)	0	0	0	0	0	0	0	0	0	33.33	3.33

- Results of the average SDR and EDR in this work very similar as the obtained by Nencioli et al. (2010) ( $SDR = 92.9\%$ ;  $EDR = 2.9\%$ )

# Eddy detection

- Decrease of the total number of eddies detected with increasing depth.

**Table 3:** Total eddies detected (cyclonic and anticyclonic) for different ocean depths for 2010

Year 2010			
Depth (m)	Total eddies	Cyclonic eddies	Anticyclonic eddies
20	1254	591	663
100	1211	645	566
250	1113	684	429
500	1027	698	329

# Eddy detection

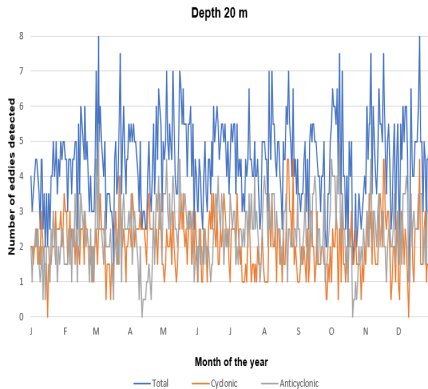


Figure 4: Annual cycle of the number of eddies detected in the Arolhos region: 20 m

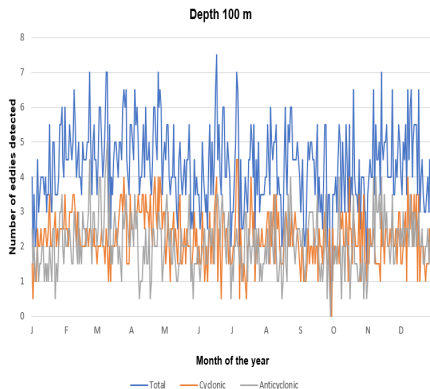


Figure 5: Annual cycle of the number of eddies detected in the Arolhos region: 100 m

# Eddy detection

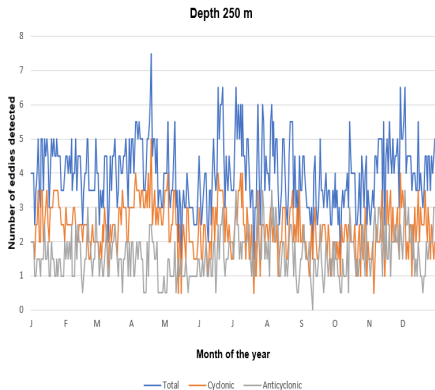


Figure 6: Annual cycle of the number of eddies detected in the Abrolhos region: 250 m

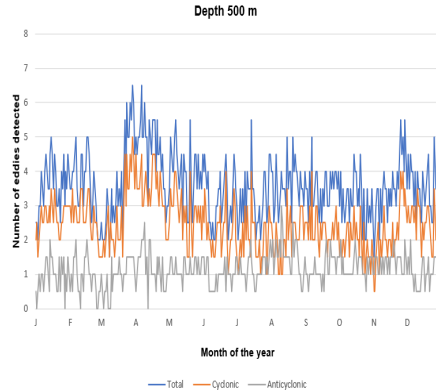


Figure 7: Annual cycle of the number of eddies detected in the Abrolhos region: 500 m

- More cyclonic eddies than anticyclonic.

# Eddy detection

Table 4: Mean coordinates of the VE, AE cyclonic and AE anticyclonic

Eddies	VE	AE cyclonic	AE anticyclonic
Latitude ( $^{\circ}$ S)	-20.4	-18.5	-18.9
Longitude ( $^{\circ}$ W)	-39.0	-37.2	-36.2

- AE anticyclonic coordinates obtained by [SOUTELINO \(2008\)](#):

Latitude ( $^{\circ}$ S) = 19.0

Longitude ( $^{\circ}$ W) = 36.5



# Eddy radius

Table 5: Eddy radius for different depths

<b>Summer 2010</b>			
<b>Depth (m)</b>	<b>Radius (km)</b>		
	VE	AE cyclonic	AE anticyclonic
20	19.8	16.7	16.7
100	40.4	35.6	16.7
250	39.9	37.9	ND
500	28.4	16.7	ND

Table 6: Eddy radius for different depths

<b>Autumn 2010</b>			
<b>Depth (m)</b>	<b>Radius (km)</b>		
	VE	AE cyclonic	AE anticyclonic
20	ND	16.7	67.9
100	ND	16.5	62.0
250	ND	16.6	54.7
500	28.4	16.8	70.1

<sup>1</sup> ND: eddy not detected

# Eddy shapes

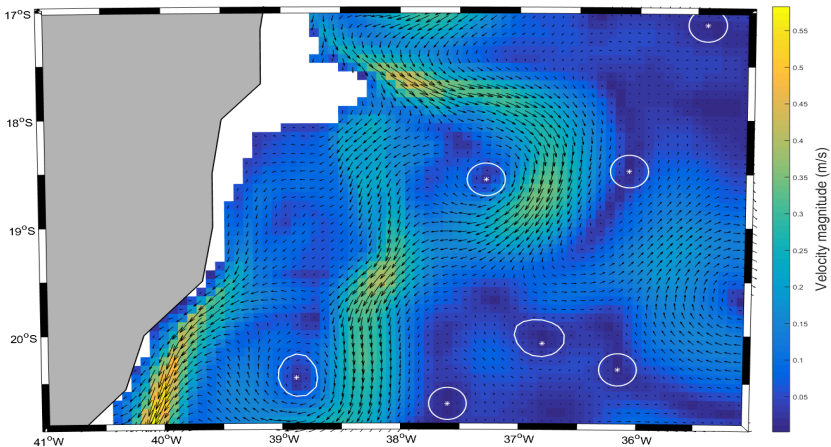


Figure 8: Mean circulation for the summer of 2010, in 20m depth.

- Small eddies: velocity fields generally characterized by stronger divergence.

# Eddy shapes

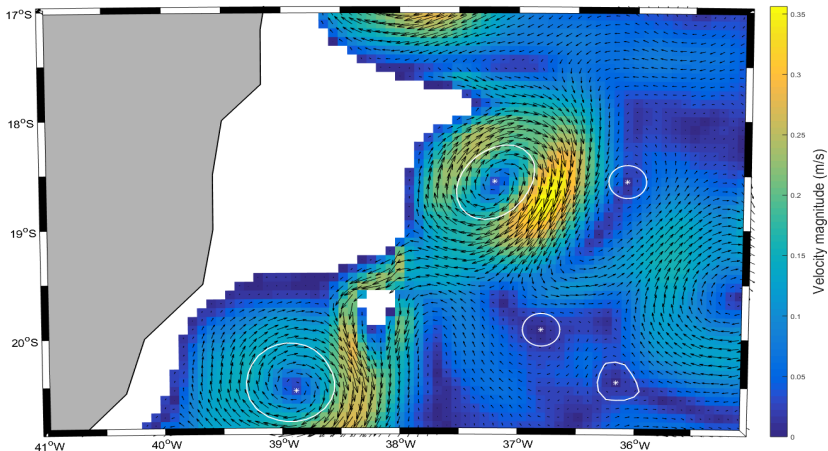


Figure 9: Mean circulation for the summer of 2010, in 100m depth.

# Eddy shapes

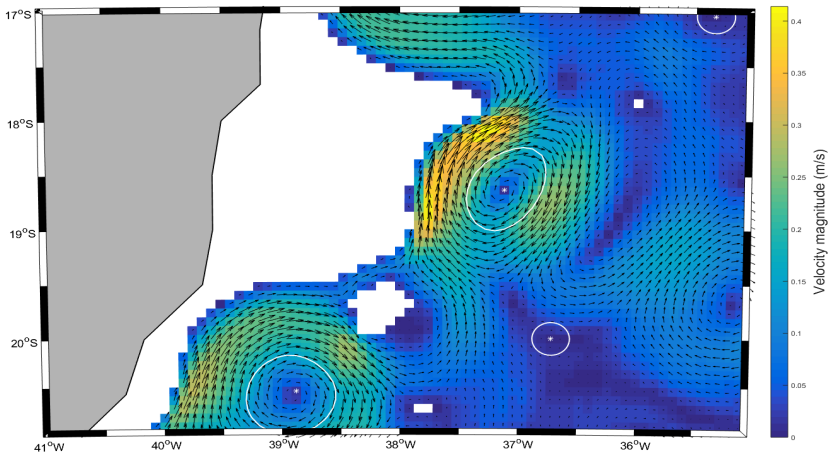


Figure 10: Mean circulation for the summer of 2010, in 250m depth.

# Eddy shapes

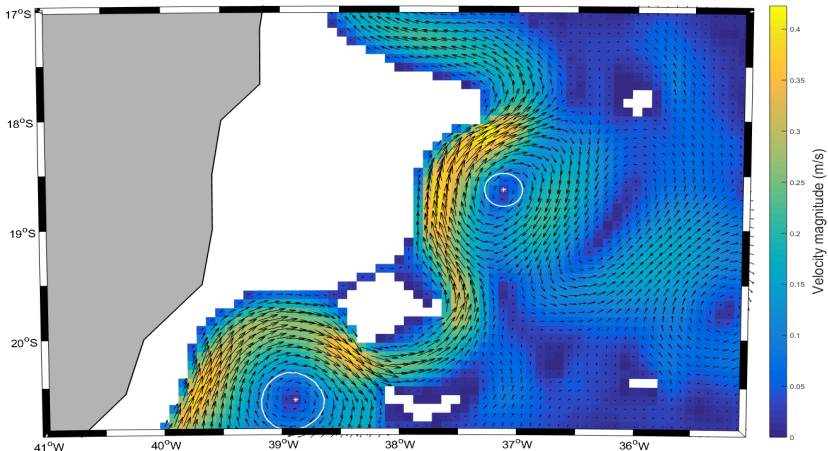


Figure 11: Mean circulation for the summer of 2010, in 500m depth.

# Eddy shapes

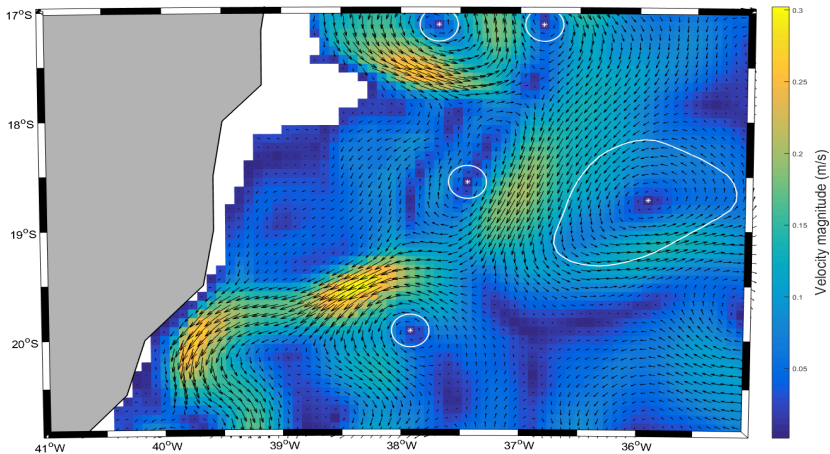


Figure 12: Mean circulation for the autumn of 2010, in 20m depth.

# Eddy shapes

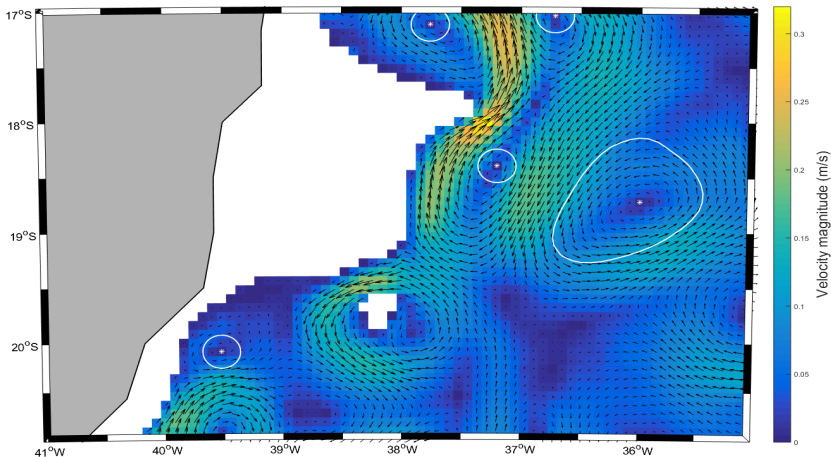


Figure 13: Mean circulation for the autumn of 2010, in 100m depth.

# Eddy shapes

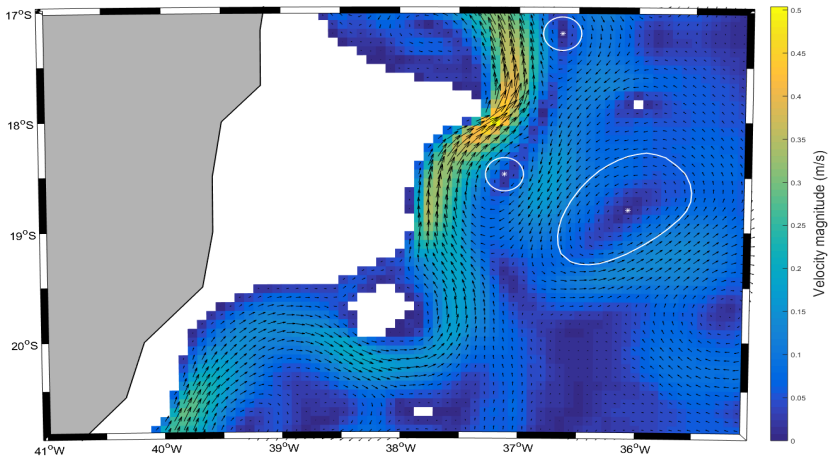


Figure 14: Mean circulation for the autumn of 2010, in 250m depth.



# Eddy shapes

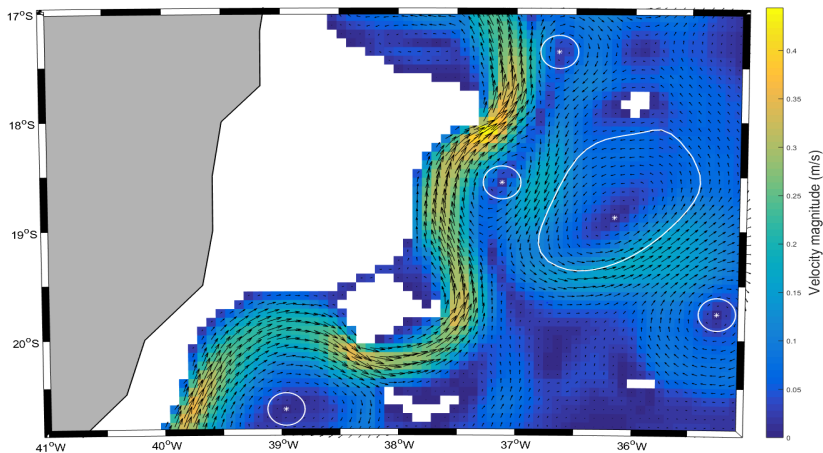


Figure 15: Mean circulation for the autumn of 2010, in 500m depth.

# Eddy tracking

**Table 7:** Number of eddies tracked and its mean lifetime, for different depths: year 2010

Year 2010		
Depth (m)	Number of eddies tracked	Mean lifetime (days)
20	277	4
100	279	4
250	200	6
500	165	7

- An increase in the mean lifetime with increasing depth.

# Eddy tracking

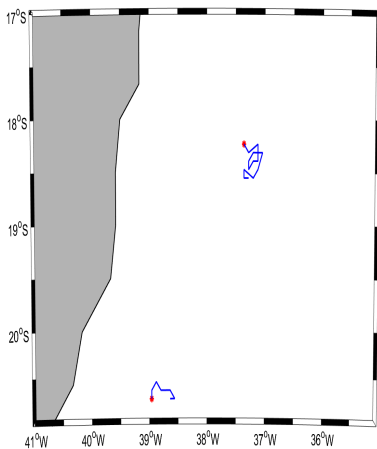


Figure 16: Eddy center tracking in the summer of 2010 for 20m

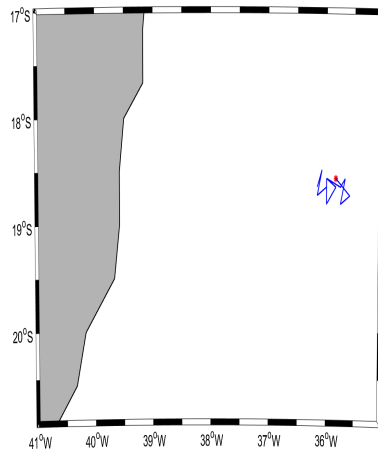


Figure 17: Eddy center tracking in the autumn of 2010 for 20m

# Conclusion

- The automated eddy detection based on the geometry of the flow proposed by [Nencioli et al. \(2010\)](#) was applied near the region of the Abrolhos Bank;
- In 250 and 500m depth, it was found the presence of more cyclonic eddies than anticyclonic.
- It was noted the increase in lifetime with increasing depth. This can be related with more EKE available in these depths ([Xia and Shen, 2015](#)).
- In our study domain, three main eddies were detected: the VE, the AE anticyclonic and the AE cyclonic.
- The summer of 2010 was the season with the VE and the AE cyclonic more defined as a eddy structure. The AE anticyclonic showed a weak structure in this season. However, the inverse occurred in the autumn, with AE anticyclonic reaching radius between 55 and 70 km and VE and AE cyclonic weaker.
- In summer, the VE and the AE cyclonic moved further east and south, respectively. In autumn, the AE anticyclonic moved further west.

# References I

- Chaigneau, A., Gizolme, A., Grados, C., et al. (2008). Mesoscale eddies off peru in altimeter records: Identification algorithms and eddy spatio-temporal patterns. *Progress in Oceanography*, 79(2):106 – 119.
- Da Silveira, I., Lima, J., Schmidt, A., Ceccopieri, W., Sartori, A., Francisco, C., and Fontes, R. (2008). **Is the meander growth in the Brazil Current system off Southeast Brazil due to baroclinic instability?** *Dynamics of Atmospheres and Oceans*, 45(3):187–207.
- de Miranda, L. B. and Castro, B. (1979). **Condições do movimento geostrófico das águas adjacentes a Cabo Frio (RJ).** *Boletim do Instituto Oceanográfico*, 28(2):79–93.
- Garfield, N. (1990). **The Brazil Current at subtropical latitudes.** PhD thesis, University of Rhode Island.
- McWilliams, J. C. (2008). The nature and consequences of oceanic eddies. *Ocean Modeling in an Eddying Regime*, pages 5–15.
- Nencioli, F., Dong, C., Dickey, T., Washburn, L., and McWilliams, J. C. (2010). A vector geometry–based eddy detection algorithm and its application to a high-resolution numerical model product and high-frequency radar surface velocities in the southern california bight. *Journal of Atmospheric and Oceanic Technology*, 27(3):564–579.
- Peterson, R. G. and Stramma, L. (1991). Upper-level circulation in the south atlantic ocean. *Progress in oceanography*, 26(1):1–73.
- Sadarjoen, I. A. (1999). *Extraction and visualization of geometries in fluid flow fields.* PhD thesis, TU Delft, Delft University of Technology.
- Schmid, C., Schäfer, H., Zenk, W., and Podestá, G. (1995). **The Vitória eddy and its relation to the Brazil Current.** *Journal of physical oceanography*, 25(11):2532–2546.
- Signorini, S. R. (1978). **On the circulation and the volume transport of the Brazil Current between the Cape of São Tomé and Guanabara Bay.** *Deep Sea Research*, 25(5):481–490.
- Soutelino, R., Gangopadhyay, A., and da Silveira, I. (2013). The roles of vertical shear and topography on the eddy formation near the site of origin of the brazil current. *Continental Shelf Research*, 70:46–60.
- SOUTELINO, R. G. (2008). **A origem da Corrente do Brasil.** Master's thesis, Instituto Oceanográfico, Universidade de São Paulo.
- Xia, Q. and Shen, H. (2015). Automatic detection of oceanic mesoscale eddies in the south china sea. *Chinese Journal of Oceanology and Limnology*, 33(5):1334–1348.

Thank you!